IsoGami: Rigid-Deployable Kirigami Materials From Isohedral Tilings

GUO HAN, ETH Zürich, Switzerland
JUAN SEBASTIAN MONTES MAESTRE, ETH Zürich, Switzerland
LOGAN NUMEROW, ETH Zürich, Switzerland
RONAN HINCHET, ETH Zürich, Switzerland
STELIAN COROS, ETH Zürich, Switzerland
BERNHARD THOMASZEWSKI, ETH Zürich, Switzerland

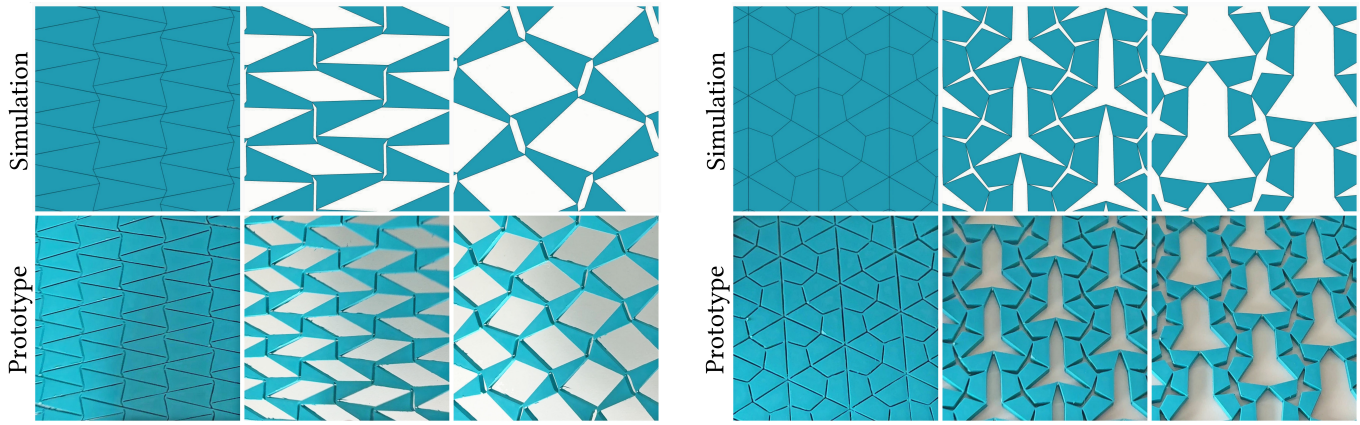

Fig. 1. We present a computational approach to explore the design space of rigid-deployable Kirigami sheets defined over isohedral tilings. *Top*: Two examples of pentagonal tilings exhibiting large tile rotations and translations during deployment. *Bottom*: Corresponding 3D-printed prototypes showing similar deployment behavior.

Rigid-deployable Kirigami sheets are unique mechanical structures, enabling extreme expansion with minimal elastic deformation. Furthermore, they unfold in fluid and coordinated motions which reveal interesting geometric patterns. Thanks to their tunable expansion behaviour, Kirigami-like structures have found a wide range of applications at various scales. However, finding the right geometry for a given application remains a significant challenge due to the complex relationship between cut patterns and deployment behavior. In this work, we introduce a computational approach to explore the design space of rigid-deployable Kirigami sheets defined over isohedral tilings, a class of periodic patterns constructed from identical polygonal tiles. Our method explores the mixed discrete-continuous design space formed by joint topologies and tile shape parameters. Leveraging tools from linkage analysis, we identify self-deployable designs with a single kinematic degree of freedom. To compute the corresponding deployment motions, we extend the concept of nonlinear compliant modes to the multi-body setting, incorporating collision handling to ensure feasible designs. Our approach enables the discovery of diverse isohedral Kirigami sheets with varying topologies, tile shapes, and expansion behavior. We showcase our results through an interactive material browser and validate selected designs with 3D-printed prototypes. Code and data for this paper are available at https://github.com/guo-han/Isogami.

CCS Concepts: • **Computing methodologies** → **Physical simulation**; *Shape modeling*.

Authors' addresses: Guo Han, ETH Zürich, Zürich, Switzerland, guohan@student.ethz.ch; Juan Sebastian Montes Maestre, ETH Zürich, Zürich, Switzerland, juansebastian.montesmaestre@inf.ethz.ch; Logan Numerow, ETH Zürich, Zürich, Switzerland, logan.numerow@inf.ethz.ch; Ronan Hinchet, ETH Zürich, Zürich, Switzerland, ronan.hinchet@srl.ethz.ch; Stelian Coros, ETH Zürich, Zürich, Switzerland, scoros@inf.ethz.ch; Bernhard Thomaszewski, ETH Zürich, Zürich, Switzerland, bthomasz@inf.ethz.ch.

1 INTRODUCTION

Through strategic placement of cuts, the ancient art of Kirigami can transform an otherwise inextensible sheet into a highly compliant mechanism. Rigid-deployable Kirigami sheets use nearly complete cuts, leaving only hinge-like connections between neighboring elements (see Fig. 1). Coordinated translation and rotation of their elements enables these rigid-deployable sheets to achieve very large expansion ratios with virtually no elastic deformation.

Thanks to their tunable expansion behavior, Kirigami materials find applications in many fields and across a wide range of scales, including healthcare [Gao et al. 2018], robotics [Jin et al. 2020a], architecture [Yin et al. 2023], and aerospace engineering [Lamoureux et al. 2015]. Despite the 3D nature of these applications, they frequently rely on 2D expansion under metric frustration. Our work focuses on this foundational mechanism, providing computational tools and insights into this core behavior. Nevertheless, finding the right Kirigami pattern for the target mechanical behaviour is challenging and laborious. The motion of the elements during deployment is nonlinear and the relationship between cut layout and expansion behavior is highly nontrivial.

In this work, we propose a new computational approach for exploring design spaces of periodic rigid-deployable Kirigami sheets. We focus on the class of isohedral tilings; identical polygonal tiles rotated and translated to form regular periodic patterns. The resulting *IsoGami* sheets are defined through a set of discrete variables—indicating the connections between tiles—and continuous parameters defining the tile shapes. The design of Kirigami sheets over isohedral tilings is therefore a mixed discrete-continuous optimization problem.

We address this problem with an approach that sequentially explores discrete topology and continuous tile shape parameters. Modeling IsoGami sheets as rigid multi-body systems allows us to leverage tools from linkage theory, including kinematic mobility, for design analysis. In particular, we propose new characterization tools based on the eigenstructure of the constraint Hessian (*i.e.* the Hessian of the penalty energy for the joint constraints). Rigid deployability implies the existence of at least one nontrivial zero eigenvalue. We focus on *self-deployable* sheets for which there is exactly one effective zero eigenvalue, with the corresponding eigenvector indicating a first-order feasible direction for deployment. To compute the full deployment trajectory from this initial direction, we extend the concept of nonlinear compliant modes [Duenser et al. 2022] to the setting of multi-body linkages. For the simulation of periodic Kirigami sheets, we use a novel formulation that permits arbitrary unit cell shapes, consisting of any number of tiles and joints including joints across unit cell boundaries. By integrating collision handling into our simulation, we are able to discard first-order feasible designs that immediately lock due to inter-tile contact.

To accelerate topology exploration, we further propose a hierarchical filtering scheme that combines feasibility checks of increasing complexity. In this way, we quickly rule out invalid designs and focus computation efforts on promising candidates.

Taken together, these tools enable us to automatically explore the design space of isohedral kirigami sheets. We showcase the resulting designs in an interactive HTML material browser included as supplementary material. This interface enables organization of designs according to various criteria, including shape and family parameters as well as different measures of expansion behavior. We furthermore provide animations of nonlinear deployment trajectories for all designs, along with corresponding expansion plots.

We demonstrate the diversity of IsoGami sheets by discussing a selection of designs with various topologies, tile shapes, and expansion behaviors. Finally, we validate the functionality of a subset of these designs with 3D-printed prototypes.

2 RELATED WORK

Mechanical Metamaterials. Metamaterials with strategically designed microstructures can produce a vast range of macromechanical properties [Bertoldi et al. 2017]. A prominent example is auxeticity, which has been identified through either geometric intuition or systematic searches of vast tessellation families [Mitschke et al. 2011]. As a real-world version of texture synthesis, the problem of designing microstructures has attracted attention from the visual computing community. The spectrum of materials is very large, ranging from 3D lattice- [Martínez et al. 2016, 2017; Panetta et al. 2015] and voxel-like materials [Schumacher et al. 2015], to multi-layer stacks [Bickel et al. 2010] and 2D structured sheet materials [Martínez et al. 2019; Schumacher et al. 2018a; Tozoni et al. 2020; Zhang et al. 2023].

Kirigami Materials. Kirigami, the ancient Japanese art of paper cutting, has emerged as a promising alternative for designing mechanical metamaterials [Czajkowski et al. 2022; Rafsanjani and Pasini 2016; Tang et al. 2017; Zhai et al. 2021]. A central challenge in this context is the design of cut layouts that lead to desired expansion behaviors. However, existing work focusing on geometry optimization relies on fixed topologies frameworks, such as quad-based patterns with predefined 4-bar connections. [Choi et al. 2021; Dudte et al. 2023]. While free-form optimization offers more flexibility [Du et al. 2024], it lacks the structural regularity of tiling-based designs. We turn instead to isohedral tilings, exploring the vast possibilities for joint topology and tile geometry that this specific space provides. Beyond metamaterials, Kirigami techniques have been explored for many applications, including inflatable structures [Jin et al. 2020b] and custom curved surfaces [Jiang et al. 2020, 2022; Konaković-Luković et al. 2018; Segall et al. 2025]. Arguably closest to our approach is the work by Liu et al. [2021], who explore Kirigami sheets defined over the so-called wallpaper group—a classification of two-dimensional repeating patterns into 17 categories. Our method explores Kirigami sheets defined over the space of isohedral tilings, which includes 93 families [Grunbaum and Shephard 1989; Kaplan 2009]. Unlike this work, we prescribe a method for exhaustive exploration of connection topologies and tile shapes within each family, and consider the impact of contact on deployment motion.

Mechanism Design. Designing functional mechanical assemblies is a challenging task that demands significant expertise, experience, and engineering knowledge. The graphics community has developed various computational tools to make this process accessible to a broader audience. For instance, one stream of works targets the synthesis of 3D-printable mechanisms that replicate the motions of virtual characters [Ceylan et al. 2013; Coros et al. 2013; Megaro et al. 2014; Zhu et al. 2012]. Prior research showed that the mobility of mechanisms can be identified through zero singular values in the constraint Jacobian matrix [Erdman et al. 2001]. Building on this concept, we develop a mobility analysis scheme for periodic kirigami mechanisms that allows us to filter out over- and under-constrained designs.

Eigenmodes in Analysis & Design. Mechanical design tasks often involve the solution of generalized eigenvalue problems. In computer graphics, this approach has found various applications, including the design of metallophones that produce specific sounds [Bharaj et al. 2015; Musialski et al. 2016; Umetani et al. 2010], enabling coarse-level simulations [Chen et al. 2017, 2019], and creating differential geometry operators [Chen et al. 2020; Liu et al. 2019] that retain desired spectral properties. Eigenvalue-based methods have also been used to design mechanical assemblies that are robust against perturbations [Liu et al. 2022b; Thomaszewski et al. 2014], 3D-printed artefacts with optimized structural performance [Schumacher et al. 2018b; Zehnder et al. 2016; Zhou et al. 2013], and bi-material distributions in the form of stripe patterns [Montes

et al. 2023]. As a common aspect of all these methods, the eigenstructure is only valid around the configuration for which it has been computed. While this limitation is acceptable if displacements remain small, it becomes a severe limitation when designing for large motions. By extending linear modes to the finite-deformation setting, nonlinear compliant modes offer an attractive solution to this problem [Duenser et al. 2022; Tang et al. 2024; Wang et al. 2024]. In essence, this approach minimizes the elastic energy of a mechanical system subject to a modal coordinate constraint, which is defined as the projection of the system's displacement onto the corresponding eigenvector. We extend this concept to the multi-body setting and propose a new algorithm that updates eigenvectors along the deployment trajectory for increased robustness.

3 METHOD

3.1 Kinematic Kirigami Model

We represent Kirigami sheets as 2D assemblies of rigid tiles connected through pin joints. Each tile $\mathcal{T}_i$ carries three degrees of freedom $\mathbf{q}_i = (\mathbf{p}_i, \theta_i)$ consisting of a rigid translation $\mathbf{p}_i = (x_i, y_i)$ and an in-plane rotation angle θ_i. The world-space coordinates of a point $\mathbf{s}$ in tile coordinates are given by

$$\mathbf{x}(\mathbf{q}_i, \mathbf{s}) = \mathbf{R}(\theta_i)\mathbf{s} + \mathbf{p}_i. \tag{1}$$

Connection Constraints. A pin joint is modeled as a constraint that two points, one on each neighboring tile, should coincide in space:

$$\mathbf{c}_{ij}(\mathbf{q}_i, \mathbf{q}_j, \mathbf{s}_k, \mathbf{s}_l) = \mathbf{x}(\mathbf{q}_i, \mathbf{s}_k) - \mathbf{x}(\mathbf{q}_j, \mathbf{s}_l) = \mathbf{0}. \tag{2}$$

Kinematically admissible configurations must satisfy all constraints, i.e., $\mathbf{c}(\mathbf{q}) = \mathbf{0}$, where $\mathbf{c}(\mathbf{q}) \in \mathbb{R}^{2m}$ stacks the constraints for all m joint connections. We enforce these conditions by minimizing a penalty function,

$$E_{\text{joints}}(\mathbf{q}) = \frac{1}{2}\mathbf{c}(\mathbf{q})^T\mathbf{c}(\mathbf{q}), \tag{3}$$

which attains its global minimum of zero when all constraints are satisfied.

Unit Cell & Periodicity. To analyze the macroscopic deployment behavior of our periodic Kirigami sheets, we consider a *unit cell* of tiles as illustrated in Fig. 2. The unit cell is chosen such that it can be tiled to fill the full plane (in the closed state) using only translations. These translations are defined by two tiling vectors $\mathbf{u}$ and $\mathbf{w}$; a tile at position $\mathbf{p}$ is replicated to $\mathbf{p} + k_u\mathbf{u} + k_w\mathbf{w}$ for all integer k_u and k_w. Note that the unit cell is not necessarily the minimal tileable unit cell, as larger unit cells permit more complex connection topologies. Joints can be placed between tiles in the same unit cell, as well as between neighboring unit cells. During deployment simulation, the full configuration of the system is given by $\mathbf{q} = [\mathbf{q}_0, \mathbf{q}_1, \ldots, \mathbf{q}_n, \mathbf{u}, \mathbf{w}]$ consisting of the tile poses $\mathbf{q}_i$ and the tiling vectors $\mathbf{u}$ and $\mathbf{w}$.

Contact. For collision handling, we include the central unit cell as well as its one-ring neighbors, *i.e.*, $k_u, k_w \in \{-1, 0, 1\}$. We prevent overlap using log-barrier penalties on vertex-edge distances similar to [Ferguson et al. 2021]. The sum of these penalties is denoted E_{coll}.

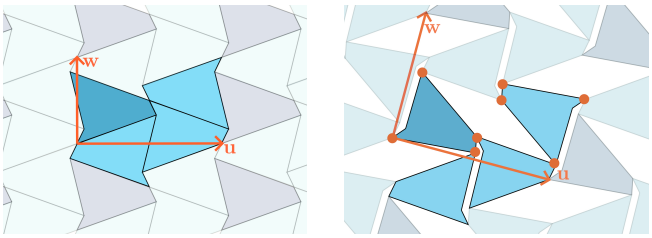

Fig. 2. An isohedral Kirigami pattern with a four-tile unit cell, in the fully closed state (*left*) and an opened state (*right*). One tile and its duplicates in neighboring unit cells are colored darker to better illustrate the pattern. Tiling vectors are drawn and labeled in blue. Additionally, a complete unit cell of joints are marked in blue on the opened state; other joints visible in the frame can be obtained by translating one of these along the tiling vectors.

3.2 Deployment Simulation

Kinematic Mobility. Our goal is to discover rigid-deployable Kirigami sheets with exactly one kinematic degree of freedom. This degree of freedom corresponds to a coordinated motion of all tiles such that pin joint constraints remain satisfied. To satisfy pin joint constraints to first order, the motion direction $\mathbf{v}$ must be orthogonal to all constraint gradients, i.e.,

$$\mathbf{J}\mathbf{v} = \frac{\partial \mathbf{c}(\mathbf{q})}{\partial \mathbf{q}}\mathbf{v} = \mathbf{0}, \tag{4}$$

where $\mathbf{J}$ is the constraint Jacobian, which is generally a non-square matrix. To compute vectors $\mathbf{v}$ satisfying the above orthogonality condition, we can use singular value decomposition. Equivalently, we perform an eigenvalue decomposition of $\mathbf{H} = \mathbf{J}^T\mathbf{J}$, which coincides with the Hessian of the constraint energy (3).

Before computing eigenvalues, we prevent rigid transformations by fixing the degrees of freedom for one tile through variable elimination. The number of remaining zero eigenvalues of $\mathbf{H}$ gives the kinematic mobility of the Kirigami sheet. We are only interested in designs that have exactly one zero eigenvalue, corresponding to self-deployable Kirigami sheets. The corresponding eigenvector $\mathbf{v}$ indicates a first-order feasible motion for the mechanism. However, due to the nonlinearity of the constraints, simply updating the state along this direction as $\mathbf{q}(t + \Delta t) = \mathbf{q}(t) + \mathbf{v}(t)\Delta t$ will violate joint constraints and introduce intersections. We next explain how to robustly compute nonlinear deployment trajectories.

Nonlinear Rigid Modes. In the continuous setting, the trajectory of a rigid-deployable structure can be described by a constrained ODE,

$$\dot{\mathbf{q}}(t) = \mathbf{v}(t), \tag{5}$$

$$s.t. \quad \mathbf{c}(\mathbf{q}(t)) = \mathbf{0}, \quad \mathbf{q}(0) = \mathbf{q}^0, \tag{6}$$

$$\mathbf{H}(\mathbf{q}(t))\mathbf{v}(t) = \mathbf{0}, \quad \mathbf{v}(t)^T\mathbf{v}(t) = 1, \tag{7}$$

Unlike conventional ODEs, the above expression corresponds to a set of differential-algebraic equations (DAEs), which are notoriously difficult to solve. To avoid this complexity, we propose a discrete time stepping scheme that robustly computes deployment trajectories by solving sequences of unconstrained minimization problems.

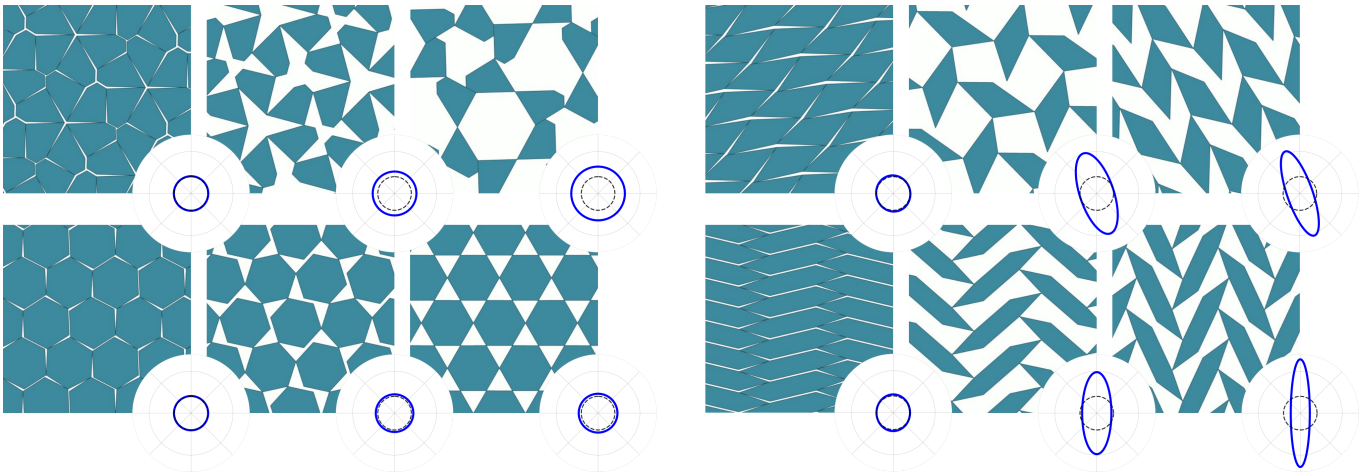

Fig. 3. Selected Isogami sheets with expansion profiles at various stages of deployment. *Left:* isotropic expansion profiles, corresponding to perfectly auxetic behaviour. *Right:* orthotropic profiles, indicating expansion along one axis and compression in the other. Blue polar plots illustrate $\mathbf{Ud}$, depicting the expansion of a unit circle into an ellipse along the principal stretch directions.

Given a state $\mathbf{q}^i$ that satisfies all joint and collision constraints, we want to compute the next state $\mathbf{q}^{i+1}$ along the deployment trajectory by stepping along the eigenvector $\mathbf{v}^i$ corresponding to the single zero eigenvalue of $\mathbf{H}(\mathbf{q}^i)$. Instead of constraining the update $\Delta\mathbf{q} = \mathbf{q}^{i+1} - \mathbf{q}^i$ to be collinear with $\mathbf{v}^i$, we ask that its projection onto the eigenvector have length β, *i.e.*, $\Delta\mathbf{q}^T\mathbf{v}^i = \beta$. This condition gives flexibility in directions orthogonal to $\mathbf{v}^i$, allowing the solution to satisfy joint and collision constraints. We formulate this constraint using a penalty function,

$$E_{\text{step}}(\mathbf{q}) = \frac{1}{2}((\mathbf{q} - \mathbf{q}^i)^T\mathbf{v}^i - \beta)^2\,, \tag{8}$$

where β is a target step length. We jointly minimize constraint and progress penalties in a single unconstrained optimization problem,

$$\mathbf{q}^{i+1} = \arg\min_{\mathbf{q}}\ E_{\text{joints}}(\mathbf{q}) + E_{\text{coll}}(\mathbf{q}) + wE_{\text{step}}(\mathbf{q}), \tag{9}$$

using an IPC-based barrier potential E_{coll} to enforce collision-free states [Ferguson et al. 2021].

The coefficient w in Eq. (9) controls the relative importance of progress and constraint terms. We use a comparatively small value $w = 10^{-4}$ to ensure that constraints are satisfied. Since the gradients of progress and constraint terms are locally orthogonal by construction, there typically exists a configuration $\mathbf{q}^{i+1}$ for which both terms are exactly zero. However, if $E_{\text{step}}(\mathbf{q}^{i+1})$ is larger than a threshold value ε for the optimized state, further action is required to determine whether we reached a turning point of the trajectory (where the eigenvector $\mathbf{v}$ changes rapidly) or the physical limit of deployment. To navigate turning points with sufficient accuracy, we successively halve the step target β until we can take a full step, *i.e.*, $E_{\text{step}}(\mathbf{q}^{i+1}) < \varepsilon$. If we cannot take a full step after 10 bisections, we conclude that no further deployment is possible.

Path Continuity at Singular Points. We do not require that the system maintain exactly one zero eigenvalue along the entire trajectory. At turning points, local degeneracies can cause multiple zero eigenvalues (typically two) to appear. In such cases, we select the direction within the null space that is most consistent with the direction from the previous step, ensuring continuity of the deployment path. Once the trajectory passes the turning point, the system generally returns to having a single zero eigenvalue corresponding to the deployment mode.

Discussion. Our approach somewhat resembles the method of Duenser et al. [2022], who compute nonlinear generalizations of eigenmodes by minimizing the elastic energy of a mechanical system in the space orthogonal to a given eigenvector. While their method sometimes yields satisfying results, it is not sufficiently robust for exploring the full deployment trajectories of Kirigami designs with large and nonlinear deployment motions. The design shown in Fig. 4 provides a clear illustration of this. In such cases, the deployment trajectory reaches a point where the dot product of the motion with the initial eigenvector vanishes. From there on, further deployment cannot be driven using the initial eigenvector. Our deployment method avoids this problem by (*a*) recomputing the eigenvector at each step, and (*b*) using an adaptive step size that ensures progress even when the eigenvector changes rapidly. See Sec. 5 for a quantitative comparison between our method and other deployment algorithms.

With a robust method for deployment simulation in hand, we can now turn to the problem of design space exploration.

4 DESIGN SPACE EXPLORATION

To design functional Kirigami sheets from isohedral tilings, we must find combinations of joint topologies and tile shape parameters that lead to deployable one-degree-of-freedom mechanisms. In general, the connection topology determines the number of degrees of freedom of the mechanism, while tile shape influences the relative movement of the tiles and determines contact. Hence, we first determine valid topologies (*i.e.* one-degree-of-freedom mechanisms) using a default tile shape for each family, where the geometry of

these default shapes is defined according to [Kaplan 2009]. We then explore variations within each valid topology by sampling tile shape parameters and computing deployment trajectories.

4.1 Topology Exploration

For each pair of adjacent tiles, we must decide whether and where to connect the two adjacent tiles with a pin joint. To avoid fixing tiles together rigidly, we may place a pin joint at either endpoint of the edge, but not both. This leads to three discrete options per edge and thus 3^m potential configurations for a unit cell with m unique edges. As we consider unit cells with up to 16 edges, the number of possible connections is generally too large for naive exhaustive exploration.

We therefore adopt a hierarchical filtering strategy that allows us to quickly rule out invalid topologies and focus resources on promising designs. A key insight is that most of this filtering can be performed before deciding on which endpoint of each edge to place a pin joint. At this stage, we must decide only whether a joint will be placed for each edge, reducing the number of distinct topologies to 2^m. The checks we perform are as follows:

(1) Each tile must have at least two neighboring tiles that are directly connected. Otherwise, the tile can rotate freely and cannot be part of a one-degree-of-freedom mechanism.
(2) All tiles in the unit cell are path-connected. We check for this by constructing a graph with n nodes, where n is the number of tiles in the unit cell, and an edge for each joint (including across unit cells). Starting from any given node, we perform BFS to check that all other nodes can be reached.
(3) All unit cells are connected. We check this by considering the *tile directions* of joints which connect neighboring unit cells. A joint between unit cell $\mathbf{k}_0 = [k_{u0}, k_{w0}]$ and unit cell $\mathbf{k}_1 = [k_{u1}, k_{w1}]$ has tile direction $\mathbf{k}_1 - \mathbf{k}_0$. There must exist joints with two linearly independent tile directions. Note that, combined with the previous condition, this implies that the tiling is *globally connected*.
(4) There cannot be three mutually neighboring tiles all connected by joints. Otherwise, these tiles are rigidly attached.

Together, these checks eliminate 99.5% of topologies in 20 ms of computation. We now expand the remaining topologies into all possible configurations of pin joints and perform further checks based on eigenanalysis:

(1) The system must have exactly one kinematic degree of freedom, as determined by mobility analysis (Sec. 3.2).
(2) We discard designs where tiles remain rigidly attached throughout the entire deployment. To ensure the structure actually opens, we require that adjacent tiles eventually separate, a condition we evaluate by checking for positive relative motion along the deployment.
(3) Due to symmetries in isohedral tilings, multiple configurations of joints may lead to the same deployment motion. We remove redundant configurations with identical motion eigenvectors.

These checks eliminate a further 99.8% of configurations in 15 minutes of computation, leaving around 7000 joint configurations for full deployment simulation. We simulate deployment to filter out configurations which cannot be expanded beyond a chosen threshold, using 54 minutes of computation time and leaving 37 interesting joint configurations for tile shape exploration.

4.2 Tile Shape Exploration

For each joint configuration with sufficient expansion during deployment, we sample a range of tile shape parameters within the corresponding isohedral tiling family. In our interactive explorer at *https://guo-han.github.io/isogami-explorer/*, we follow the classification in [Kaplan 2009], labeling tiling families as IH# and shape parameters as v#. We systematically explore permutations of these parameters within each family. We sample over a coarse grid in parameter space, selecting ranges of parameters which lead to well-shaped tiles (non-intersecting, closed tile geometries). This process is largely heuristic and could benefit from further automation. Tiling families have no more than 6 shape parameters, and we sample a total of 2787 different patterns across family, shape parameter and joint configuration. Of these, 846 achieve the desired threshold for expansion ratio and are included in the material browser. This complete exploration requires 6 hours and 45 minutes of computation time.

4.3 Characterizing Kirigami Sheets

To concisely quantify the mechanical behavior of our designs, we analyze the directional expansion of each design under deployment. To this end, we compute the macroscopic deformation gradient of the unit cell as the linear map that transforms initial (closed-state) tiling vectors to their deployed (open-state) counterparts as

$$[\mathbf{u}\ \mathbf{w}] = \mathbf{F}[\bar{\mathbf{u}}\ \bar{\mathbf{w}}]\,, \tag{10}$$

where $\bar{\mathbf{u}}$ and $\bar{\mathbf{w}}$ represent the closed-state tiling vectors. For a unit vector $\mathbf{d} \in \mathbb{R}^2$, the corresponding directional expansion is computed as $\varepsilon(\theta) = \mathbf{d}^T(\mathbf{U} - \mathbf{I})\mathbf{d}$, where $\mathbf{U}$ is the right stretch tensor from the polar decomposition $\mathbf{F} = \mathbf{R}\mathbf{U}$.

To characterize a given Kirigami design, we provide plots of minimum and maximum expansion values as a function of the deployment parameter t , defined as the normalized arc length along the state-space trajectory from initialization ($t = 0$) to full deployment ($t = 1$). We furthermore display the directional expansion profile for a chosen t as a polar plot. See Fig. 3 and our HTML material browser for examples.

5 RESULTS

We use the approach detailed in Sec. 4 to explore the design space of rigid-deployable Kirigami sheets defined over 34 families of isohedral tilings. Our automated filtering and sampling process returns 846 functional Kirigami sheets, indicating a rich and diverse design space. In the following, we present and analyze a selection of Kirigami designs. The complete set of functional designs can be explored using our interactive material browser included as supplementary material.

Deployment Simulation. Being able to robustly compute full deployment trajectories for arbitrary designs is a crucial ingredient for automatic exploration of Kirigami material spaces. To illustrate the advantages of our proposed deployment algorithm, we compare

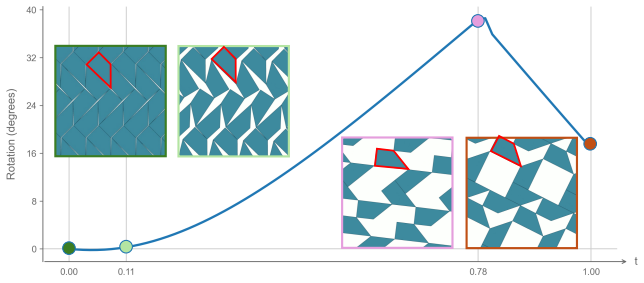

Fig. 4. Comparison of deployment algorithms on a given kirigami design. The rotation of a selected tile (outlined in *red*) is plotted along the deployment trajectory. Colored dots indicated end-of-trajectory points for the spring-based opening method (*light green*), nonlinear compliant modes (*purple*), and our method (*orange*). Only our method is able to fully open the design.

its behavior with existing alternatives. Our first baseline is the expansion method by Liu et al. [2022a] which uses springs attached to selected elements to pull the structure into an open state. For the example pattern shown in Fig. 4, this method achieves a final deployment parameter $t = 0.11$ relative to the deployment limit $t = 1.0$. The method of nonlinear compliant modes [Duenser et al. 2022] further expands the structure to $t = 0.78$. Ours is the only method to achieve the physical limit of deployment $t = 1.0$, at which point further motion is prevented by inter-tile contact.

Expansion Ratios. One characteristic feature of rigid-deployable Kirigami sheets is the widely-varying directional expansion during deployment. Designs with threefold rotational symmetry exhibit perfectly isotropic deployment with equal expansion ratios in all directions, corresponding to ideal auxetic behavior; other designs exhibit extreme orthotropic deformation, with positive Poisson's ratio and large expansion along one direction throughout most of the deployment trajectory. Examples of both are presented in Fig. 3.

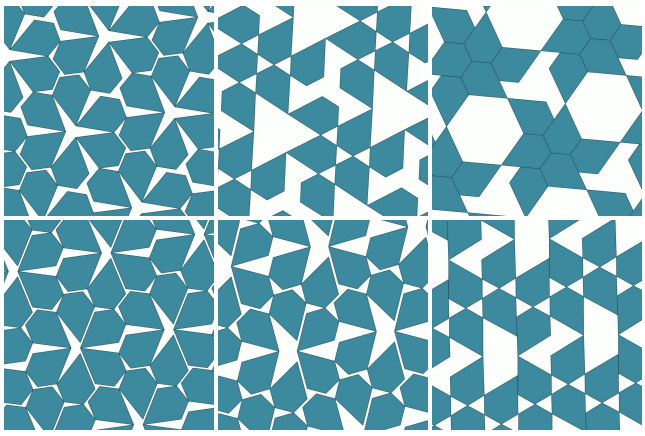

Fig. 5. Two unique Isogami materials, resulting from different joint topologies on the same periodic tiling. Each has a unit cell consisting of six tiles and nine joints.

Contact. As part of our deployment simulation algorithm, we detect and resolve contact between tiles. In all observed examples, contact has an effect only when blocking further expansion of the sheet, terminating the deployment trajectory. We expect that it is possible for rigid or sliding contact to provide one or more of the necessary constraints to reach one degree of freedom; however, we do not observe this in any of our designs.

Impact of Topology and Tile Shape. Different joint topologies and tile shapes within the same isohedral tiling family give substantially different deployment behaviors. See Fig. 5 for an example of two interesting topologies drawn from the same periodic tiling. We encourage the reader to explore different designs in our material browser to best experience these effects.

5.1 Topological Diversity & Linkage Analysis

To gain deeper insight into the behavior of our Isogami materials, we analyze the results produced by our sampling method through the lens of linkage identification. Any valid topology defined over a unit cell of tiles induces a set of planar linkages, *i.e.*, closed loops of bars connected between joints. The number and types of linkages spanning the unit cell largely determines the generic behavior of the material.

To characterize the diversity of topologies in our dataset, we process all designs and automatically determine their linkage types. To this end, we construct a graph representation of a patch consisting of the central unit cell and its one-ring neighbors, where nodes represent tiles and edges represent joints (ignoring joints which connect to tiles outside this patch). In this representation, linkages correspond to chordless (induced) cycles—loops of nodes without shortcuts, meaning that no two nodes in the cycle are connected by an edge outside the cycle. We detect all chordless cycles in the graph, then remove periodic duplicates to obtain a tileable unit cell of linkages. This analysis identifies all linkage types across the complete data set in a few seconds.

Fig. 6 provides an overview of the linkage types detected in this way. Many topologies lead to combinations of two to four 4-bar linkages (Fig. 6f). Many interesting cases involve 6-bar linkages, arranged around degree-6 vertices or clustered degree-3 vertices in compactly folded star-shaped configurations, enabling large expansion ratios (Fig. 6c, 6d, 6e).

Less common are linkages with five, eight, and ten bars. For example, one design combines an 8-bar linkage with two 5-bar linkages (Fig. 6b). Another notable example features two 4-bar linkages alongside a 10-bar linkage (Fig. 6a). Interestingly, linkages sometimes contain more tiles than there are tiles in the unit cell; this 10-bar linkage example has a unit cell of 6 tiles, and the linkage traverses several unit cells.

Tile Degree. The vast majority of patterns consists of degree-3 tiles, *i.e.*, each tile connects to three neighbors. Exceptions include families based on regular quad-grids (Fig. 6f), where all tiles have degree four. An unusual case is the hexagonal pattern with sixfold symmetric tiles, for which our exploration algorithm found a topology interleaving degree-3 and degree-6 tiles. This pattern,

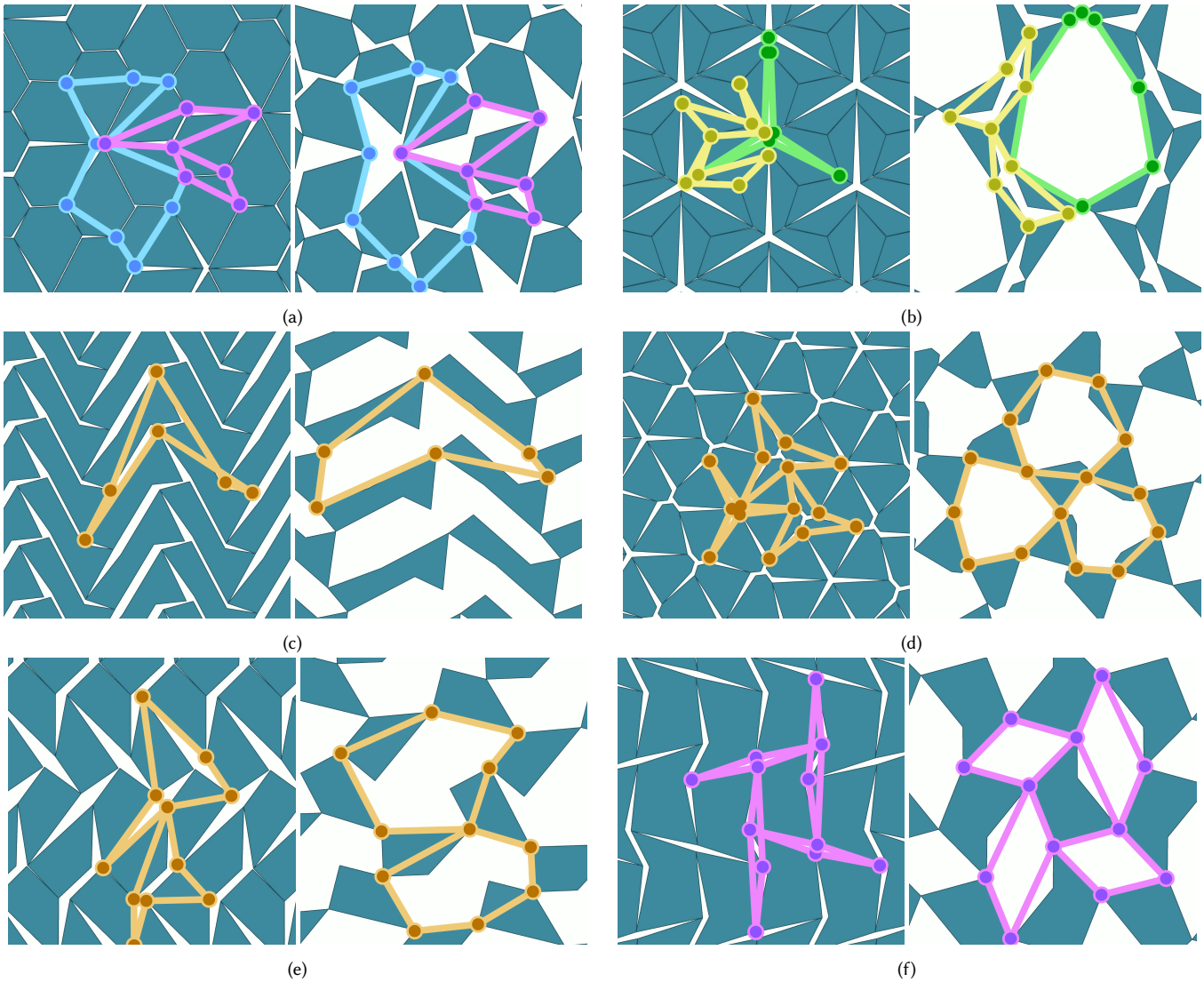

Fig. 6. The motion of any Kirigami sheet can be viewed through the lens of a corresponding planar linkage mechanism. Each subfigure depicts one unit cell of linkages for a given Isogami pattern in a closed (*left*) and deployed (*right*) state. Linkages are colored by number of bars; these examples contain 4- (purple), 5- (yellow), 6- (orange), 8- (green) and 10-bar (blue) linkages.

shown in Fig. 3 (*bottom left*), reaches a fully-closed state at the end of deployment with tiles rotated by 120 degrees.

5.2 3D-printed Prototypes

To demonstrate the feasibility of our IsoGami designs, we 3D-printed a set of samples for selected patterns. Results are shown in Fig. 1 and Fig. 7; please refer to the accompanying video for a side-by-side comparison between printed samples and corresponding simulations. Instead of using pin joints, we 3D printed thin lamella-like polypropylene connections between corresponding tiles. While the elasticity of these connections naturally resists deformations, the prototypes can nevertheless be opened without significant effort. However, achieving full deployment of designs that exhibit very large tile rotations—such as the hexagon pattern shown in Fig. 3 (*bottom left*), which possesses a second closed state different from its rest state—is likely not possible with this simplified manufacturing approach.

5.3 Performance & Statistics

The complete design exploration process and database generation from scratch requires 8 hours of computation.

The simulation time to generate a single deployment trajectory depends on how much a pattern can be expanded and the number of tiles within the unit cell. The average simulation time is 0.03 seconds per frame and 1.40 seconds per complete trajectory, up to a maximum of 6.5 seconds for patterns in family IH30.

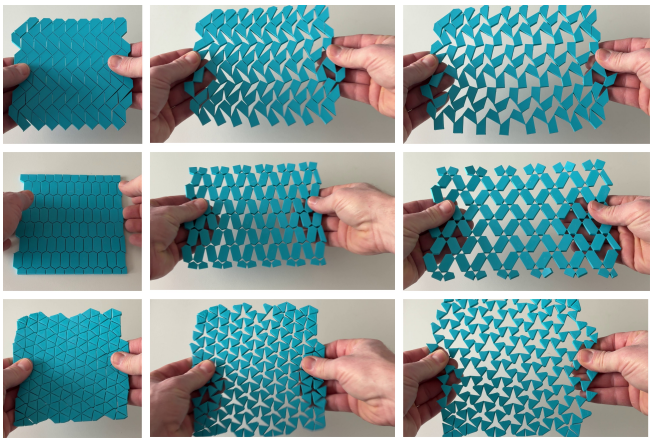

Fig. 7. 3D-printed prototypes for three Isogami designs in closed (*left*) and opened (*right*) configurations.

6 CONCLUSIONS

We presented a method for exploring the space of rigid-deployable Kirigami sheets made from periodic tilings. In particular, we developed tools that exploit the eigenstructure of Kirigami sheets to analyze their kinematic mobility. We extended the method of nonlinear compliant modes [Duenser et al. 2022] to the multi-body setting to yield complete nonlinear deployment trajectories. Finally, we presented exploration strategies for efficient discovery of valid connection topologies, including a hierarchical filtering strategy which operates in a reduced topology space to quickly and efficiently eliminate the vast majority of invalid designs.

Limitations and Future Work. We perform topology screening using default tile shapes. Although we cannot rule out the possibility that geometry affects the Jacobian spectrum and the number of zero eigenvalues, such instances were rare. Using fixed shapes thus provides an efficient trade-off, though exhaustive shape-aware topology exploration remains an area for future work. Our method applies to periodic Kirigami designs, which have many applications in arts and engineering. Nevertheless, extending our work to graded patterns and non-periodic materials is an exciting direction for future work. Beyond isohedral tilings, there are many other types of parametric pattern spaces that could be worth exploring. Non-identical tile shapes should pose no problem in principle, but larger unit cells and the corresponding increase in possible topologies will rapidly become a bottle neck. To address this combinatorial explosion, it would be interesting to explore methods for more constrained exploration of topologies. For inverse design, direct gradient-based methods often fail to traverse topological changes in the design space. Our framework provides good initializations by selecting high-quality candidates from enumerated designs, which can be further refined via local geometric optimization as in prior work [Schumacher et al. 2018a]. While full inverse design is beyond our scope, this two-stage strategy—global screening followed by local refinement—offers a promising direction. Finally, even though we have focused on rigid-deployable materials, extension to materials with strategically placed deformable tiles or joints would open the door to multistable Kirigami sheets.

ACKNOWLEDGMENTS

We thank the reviewers for their valuable feedback. This work was supported by the Swiss National Science Foundation through SNF project grant 200021-236469.

REFERENCES

Katia Bertoldi, Vincenzo Vitelli, Johan Christensen, and Martin Van Hecke. 2017. Flexible mechanical metamaterials. *Nature Reviews Materials* 2, 11 (2017), 1–11.

Gaurav Bharaj, David I. W. Levin, James Tompkin, Yun Fei, Hanspeter Pfister, Wojciech Matusik, and Changxi Zheng. 2015. Computational Design of Metallophone Contact Sounds. *ACM Trans. Graph.* 34, 6, Article 223 (Oct. 2015), 13 pages. https://doi.org/10.1145/2816795.2818108

Bernd Bickel, Moritz Bächer, Miguel A Otaduy, Hyunho Richard Lee, Hanspeter Pfister, Markus Gross, and Wojciech Matusik. 2010. Design and fabrication of materials with desired deformation behavior. *ACM Transactions on Graphics (TOG)* 29, 4 (2010), 1–10.

Duygu Ceylan, Wilmot Li, Niloy J Mitra, Maneesh Agrawala, and Mark Pauly. 2013. Designing and fabricating mechanical automata from mocap sequences. *ACM Transactions on Graphics (TOG)* 32, 6 (2013), 1–11.

Desai Chen, David I. W. Levin, Wojciech Matusik, and Danny M. Kaufman. 2017. Dynamics-Aware Numerical Coarsening for Fabrication Design. *ACM Trans. Graph.* 36, 4, Article 84 (jul 2017), 15 pages. https://doi.org/10.1145/3072959.3073669

Honglin Chen, Hsueh-TI Derek Liu, Alec Jacobson, and David I. W. Levin. 2020. Chordal Decomposition for Spectral Coarsening. *ACM Trans. Graph.* 39, 6, Article 265 (nov 2020), 16 pages. https://doi.org/10.1145/3414685.3417789

Yu Ju (Edwin) Chen, David I. W. Levin, Danny Kaufmann, Uri Ascher, and Dinesh K. Pai. 2019. EigenFit for Consistent Elastodynamic Simulation across Mesh Resolution. In *Proceedings of the 18th Annual ACM SIGGRAPH/Eurographics Symposium on Computer Animation* (Los Angeles, California) *(SCA '19)*. Association for Computing Machinery, New York, NY, USA, Article 5, 13 pages. https://doi.org/10.1145/3309486.3340248

Gary PT Choi, Levi H Dudte, and L Mahadevan. 2021. Compact reconfigurable kirigami. *Physical Review Research* 3, 4 (2021), 043030.

Stelian Coros, Bernhard Thomaszewski, Gioacchino Noris, Shinjiro Sueda, Moira Forberg, Robert W. Sumner, Wojciech Matusik, and Bernd Bickel. 2013. Computational design of mechanical characters. *ACM Trans. Graph.* 32, 4, Article 83 (July 2013), 12 pages. https://doi.org/10.1145/2461912.2461953

Michael Czajkowski, Corentin Coulais, Martin van Hecke, and D. Zeb Rocklin. 2022. Conformal elasticity of mechanism-based metamaterials. *Nature Communications* 13 (12 2022). Issue 1. https://doi.org/10.1038/s41467-021-27825-0

Chen Du, Yiqiang Wang, and Zhan Kang. 2024. Cut layout optimization for design of kirigami metamaterials under large stretching. *Theoretical and Applied Mechanics Letters* (2024), 100528. https://doi.org/10.1016/j.taml.2024.100528

Levi H Dudte, Gary PT Choi, Kaitlyn P Becker, and L Mahadevan. 2023. An additive framework for kirigami design. *Nature Computational Science* 3, 5 (2023), 443–454.

Simon Duenser, Bernhard Thomaszewski, Roi Poranne, and Stelian Coros. 2022. Nonlinear Compliant Modes for Large-deformation Analysis of Flexible Structures. *ACM Trans. Graph.* 42, 2, Article 21 (Nov. 2022), 11 pages. https://doi.org/10.1145/3568952

Arthur G.. Erdman, George N.. Sandor, and Sridhar Kota. 2001. *Mechanism design: analysis and synthesis.* Prentice Hall.

Zachary Ferguson, Minchen Li, Teseo Schneider, Francisca Gil-Ureta, Timothy Langlois, Chenfanfu Jiang, Denis Zorin, Danny M. Kaufman, and Daniele Panozzo. 2021. Intersection-free Rigid Body Dynamics. *ACM Transactions on Graphics (SIGGRAPH)* 40, 4, Article 183 (2021).

Bingbing Gao, Abdelrahman Elbaz, Zhenzhu He, Zhuoying Xie, Hua Xu, Songqin Liu, Enben Su, Hong Liu, and Zhongze Gu. 2018. Bioinspired kirigami fish-based highly stretched wearable biosensor for human biochemical–physiological hybrid monitoring. *Advanced Materials Technologies* 3, 4 (2018), 1700308.

Branko Grunbaum and Geoffrey Colin Shephard. 1989. *Tilings and patterns: An introduction.* WH Freeman and Company.

Caigui Jiang, Florian Rist, Helmut Pottmann, and Johannes Wallner. 2020. Freeform quad-based kirigami. *ACM Transactions on Graphics (TOG)* 39, 6 (2020), 1–11.

Caigui Jiang, Florian Rist, Hui Wang, Johannes Wallner, and Helmut Pottmann. 2022. Shape-morphing mechanical metamaterials. *Computer-Aided Design* 143 (2022), 103146.

Lishuai Jin, Antonio Elia Forte, Bolei Deng, Ahmad Rafsanjani, and Katia Bertoldi. 2020a. Kirigami-inspired inflatables with programmable shapes. *Advanced Materials* 32, 33 (2020), 2001863.

Lishuai Jin, Antonio Elia Forte, Bolei Deng, Ahmad Rafsanjani, and Katia Bertoldi. 2020b. Kirigami-Inspired Inflatables with Programmable Shapes. *Advanced*

Materials 32, 33 (2020), 2001863. https://doi.org/10.1002/adma.202001863 arXiv:https://onlinelibrary.wiley.com/doi/pdf/10.1002/adma.202001863

Craig Kaplan. 2009. *Introductory Tiling Theory for Computer Graphics* (1st ed.). Morgan and Claypool Publishers.

Mina Konaković-Luković, Julian Panetta, Keenan Crane, and Mark Pauly. 2018. Rapid Deployment of Curved Surfaces via Programmable Auxetics. *ACM Trans. Graph.* 37, 4, Article 106 (July 2018), 13 pages. https://doi.org/10.1145/3197517.3201373

Aaron Lamoureux, Kyusang Lee, Matthew Shlian, Stephen R Forrest, and Max Shtein. 2015. Dynamic kirigami structures for integrated solar tracking. *Nature communications* 6, 1 (2015), 8092.

Hsueh-Ti Derek Liu, Alec Jacobson, and Maks Ovsjanikov. 2019. Spectral Coarsening of Geometric Operators. *ACM Trans. Graph.* 38, 4, Article 105 (jul 2019), 13 pages. https://doi.org/10.1145/3306346.3322953

Lucy Liu, Gary PT Choi, and L Mahadevan. 2022a. Quasicrystal kirigami. *Physical Review Research* 4, 3 (2022), 033114.

Lucy Liu, Gary P. T. Choi, and L. Mahadevan. 2021. Wallpaper group kirigami. *Proceedings of the Royal Society A: Mathematical, Physical and Engineering Sciences* 477, 2252 (2021), 20210161. https://doi.org/10.1098/rspa.2021.0161 arXiv:https://royalsocietypublishing.org/doi/pdf/10.1098/rspa.2021.0161

Zhenyuan Liu, Jingyu Hu, Hao Xu, Peng Song, Ran Zhang, Bernd Bickel, and Chi-Wing Fu. 2022b. Worst-Case Rigidity Analysis and Optimization for Assemblies with Mechanical Joints. In *Computer Graphics Forum*, Vol. 41. Wiley Online Library, 507–519.

Jonàs Martínez, Jérémie Dumas, and Sylvain Lefebvre. 2016. Procedural voronoi foams for additive manufacturing. *ACM Transactions on Graphics (TOG)* 35, 4 (2016), 1–12.

Jonàs Martínez, Mélina Skouras, Christian Schumacher, Samuel Hornus, Sylvain Lefebvre, and Bernhard Thomaszewski. 2019. Star-shaped metrics for mechanical metamaterial design. *ACM Transactions on Graphics (TOG)* 38, 4 (2019), 1–13.

Jonàs Martínez, Haichuan Song, Jérémie Dumas, and Sylvain Lefebvre. 2017. Orthotropic k-nearest foams for additive manufacturing. *ACM Transactions on Graphics (TOG)* 36, 4 (2017), 1–12.

Vittorio Megaro, Bernhard Thomaszewski, Damien Gauge, Eitan Grinspun, Stelian Coros, and Markus H Gross. 2014. ChaCra: An Interactive Design System for Rapid Character Crafting.. In *Symposium on Computer Animation*. 123–130.

Holger Mitschke, Jan Schwerdtfeger, Fabian Schury, Michael Stingl, Carolin Körner, Robert F Singer, Vanessa Robins, Klaus Mecke, and Gerd E Schröder-Turk. 2011. Finding auxetic frameworks in periodic tessellations. *Advanced Materials* 23, 22-23 (2011), 2669–2674.

Juan Montes, Yinwei Du, Ronan Hinchet, Stelian Coros, and Bernhard Thomaszewski. 2023. Differentiable Stripe Patterns for Inverse Design of Structured Surfaces. *ACM Transactions on Graphics (TOG)* (2023).

Przemyslaw Musialski, Christian Hafner, Florian Rist, Michael Birsak, Michael Wimmer, and Leif Kobbelt. 2016. Non-linear Shape Optimization Using Local Subspace Projections. *ACM Trans. Graph.* 35, 4, Article 87 (July 2016), 13 pages. https://doi.org/10.1145/2897824.2925886

Julian Panetta, Qingnan Zhou, Luigi Malomo, Nico Pietroni, Paolo Cignoni, and Denis Zorin. 2015. Elastic textures for additive fabrication. *ACM Transactions on Graphics (TOG)* 34, 4 (2015), 1–12.

Ahmad Rafsanjani and Damiano Pasini. 2016. Bistable auxetic mechanical metamaterials inspired by ancient geometric motifs. *Extreme Mechanics Letters* 9 (2016), 291–296.

Christian Schumacher, Bernd Bickel, Jan Rys, Steve Marschner, Chiara Daraio, and Markus Gross. 2015. Microstructures to control elasticity in 3D printing. *ACM Transactions on Graphics (Tog)* 34, 4 (2015), 1–13.

Christian Schumacher, Steve Marschner, Markus Gross, and Bernhard Thomaszewski. 2018a. Mechanical characterization of structured sheet materials. *ACM Transactions on Graphics (TOG)* 37, 4 (2018), 1–15.

Christian Schumacher, Jonas Zehnder, and Moritz Bächer. 2018b. Set-in-stone: worst-case optimization of structures weak in tension. *ACM Trans. Graph.* 37, 6, Article 252 (Dec. 2018), 13 pages. https://doi.org/10.1145/3272127.3275085

Aviv Segall, Jing Ren, Marcel Padilla, and Olga Sorkine-Hornung. 2025. Reconfigurable Hinged Kirigami Tessellations. In *Proceedings of the SIGGRAPH Asia 2025 Conference Papers (SA Conference Papers '25)*. Association for Computing Machinery, New York, NY, USA, Article 99, 11 pages. https://doi.org/10.1145/3757377.3763895

Pengbin Tang, Ronan Hinchet, Roi Poranne, Bernhard Thomaszewski, and Stelian Coros. 2024. Modal Folding: Discovering Smooth Folding Patterns for Sheet Materials using Strain-Space Modes. In *ACM SIGGRAPH 2024 Conference Papers* (Denver, CO, USA) *(SIGGRAPH '24)*. Association for Computing Machinery, New York, NY, USA, Article 48, 9 pages. https://doi.org/10.1145/3641519.3657401

Yichao Tang, Gaojian Lin, Shu Yang, Yun Kyu Yi, Randall D. Kamien, and Jie Yin. 2017. Programmable Kiri-Kirigami Metamaterials. *Advanced Materials* 29, 10 (2017), 1604262. https://doi.org/10.1002/adma.201604262 arXiv:https://onlinelibrary.wiley.com/doi/pdf/10.1002/adma.201604262

Bernhard Thomaszewski, Stelian Coros, Damien Gauge, Vittorio Megaro, Eitan Grinspun, and Markus Gross. 2014. Computational Design of Linkage-Based Characters. *ACM Trans. Graph.* 33, 4, Article 64 (July 2014), 9 pages. https://doi.org/10.1145/2601097.2601143

Davi Colli Tozoni, Jérémie Dumas, Zhongshi Jiang, Julian Panetta, Daniele Panozzo, and Denis Zorin. 2020. A low-parametric rhombic microstructure family for irregular lattices. *ACM Transactions on Graphics (TOG)* 39, 4 (2020), 101–1.

Nobuyuki Umetani, Jun Mitani, and Takeo Igarashi. 2010. Designing Custom-made Metallophone with Concurrent Eigenanalysis. In *Proceedings of the International Conference on New Interfaces for Musical Expression*. Zenodo, 26–30. https://doi.org/10.5281/zenodo.1177917

Jiahong Wang, Yinwei Du, Stelian Coros, and Bernhard Thomaszewski. 2024. Neural Modes: Self-supervised Learning of Nonlinear Modal Subspaces. In *Proceedings of the IEEE/CVF Conference on Computer Vision and Pattern Recognition*. 23158–23167.

Hanzhi Yin, Xishu Zhou, Zhengui Zhou, Rong Liu, Xiwei Mo, Zewen Chen, Erqi Yang, Zhen Huang, Hao Li, Hao Wu, et al. 2023. Switchable kirigami structures as window envelopes for energy-efficient buildings. *Research* 6 (2023), 0103.

Jonas Zehnder, Stelian Coros, and Bernhard Thomaszewski. 2016. Designing structurally-sound ornamental curve networks. *ACM Trans. Graph.* 35, 4, Article 99 (July 2016), 10 pages. https://doi.org/10.1145/2897824.2925888

Zirui Zhai, Lingling Wu, and Hanqing Jiang. 2021. Mechanical metamaterials based on origami and kirigami. Issue 4. https://doi.org/10.1063/5.0051088

Zhan Zhang, Christopher Brandt, Jean Jouve, Yue Wang, Tian Chen, Mark Pauly, and Julian Panetta. 2023. Computational Design of Flexible Planar Microstructures. *ACM Trans. Graph.* 42, 6, Article 185 (dec 2023), 16 pages. https://doi.org/10.1145/3618396

Qingnan Zhou, Julian Panetta, and Denis Zorin. 2013. Worst-case structural analysis. *ACM Trans. Graph.* 32, 4 (2013), 137–1.

Lifeng Zhu, Weiwei Xu, John Snyder, Yang Liu, Guoping Wang, and Baining Guo. 2012. Motion-guided mechanical toy modeling. *ACM Transactions on Graphics (TOG)* 31, 6 (2012), 1–10.